arXiv:1407.1721v1 [nucl-th] 7 Jul 2014

Low-energy magnetic radiation: deviations from GOE[1]

S. Frauendorf*, R. Schwengner† and K. Wimmer**

*University Notre Dame, IN 46557, USA
†IRP, HZDR, 01328 Dresden, Germany
**Central Michigan University, Mt. Pleasant, MI 48859, USA

Abstract. A pronounced spike at low energy in the strength function for magnetic radiation (LEMAR) is found by means of Shell Model calculations, which explains the experimentally observed enhancement of the dipole strength. LEMAR originates from statistical low-energy M1-transitions between many excited complex states. Re-coupling of the proton and neutron high-j orbitals generates the strong magnetic radiation. LEMAR is closely related to Magnetic Rotation. LEMAR is predicted for nuclides participating in the r-process of element synthesis and is expected to change the reaction rates. An exponential decrease of the strength function and a power law for the size distribution of the $B(M1)$ values are found, which strongly deviate from the ones of the GOE of random matrices, which is commonly used to represent complex compound states.

Keywords: Shell Model, M1 strength function, magnetic rotation, Gaussian Orthogonal Ensemble

LOW-ENERGY ENHANCEMENT OF GAMMA RADIATION

Photonuclear reactions and the inverse radiative-capture reactions between nuclear states in the region of high excitation energy and large level density are of considerable interest in many applications. Radiative neutron capture, for example, plays a central role in the synthesis of the elements in various stellar environments, for next-generation nuclear technologies, and as the transmutation of long-lived nuclear waste. A critical input to calculations of the reaction rates is the average strength of the cascade of γ-transitions de-exciting the nucleus, which is described by photon strength function. Modifications of its low-energy part can cause drastic changes in the abundances of elements produced via neutron capture in the r-process occurring in violent stellar events [2]. Such an increase of the dipole strength function below 3 MeV toward low γ-ray energy has recently been observed in nuclides in the mass range from $A \approx$ 40 to 100. In particular, this low-energy enhancement of the strength function was deduced from experiments using (^{3}He,^{3}He') reactions on various Mo isotopes [3]. The (^{3}He,^{3}He') data for ^{94}Mo are shown in Fig. 1 (left). Around 1 MeV, the experimental strength function (blue) is about a factor of 10 larger than expected for a damped Giant Dipole Resonance shown by the dashed green curve, which is calculated by the standard GLO expression commonly used for describing the strength of electric dipole (E1) radiation in this energy region.

The enhancement is not observed in the inverse process of absorbing γ-quanta by nuclei in the ground state. Only few discrete lines are found within the interval of the first 4 MeV [4]. The enhancement in the de-excitation cascade must be related to the complex structure of the highly excited states among which the transitions occur. Fig. 1 (right) shows the summed reduced probabilities of all discrete transitions reported for the nuclides with $88 \leq A \leq 98$ depending on their transition energy. The reduced probabilities of the magnetic transitions $B(M1)$ clearly increase toward zero transition energy, whereas no such tendency is seen for reduced probabilities $B(E1)$ for the electric transitions. Based on this observation we conjectured that the enhancement seen in experiments like the one in Fig. 1 (left) is caused by $M1$ transitions between high-lying states. To study this conjecture, we carried out Shell Model calculations for the nuclides ^{94,95,96}Mo and ^{90}Zr, for which the enhancement has been observed in experiment.

[1] Part of the material has been published in [1]

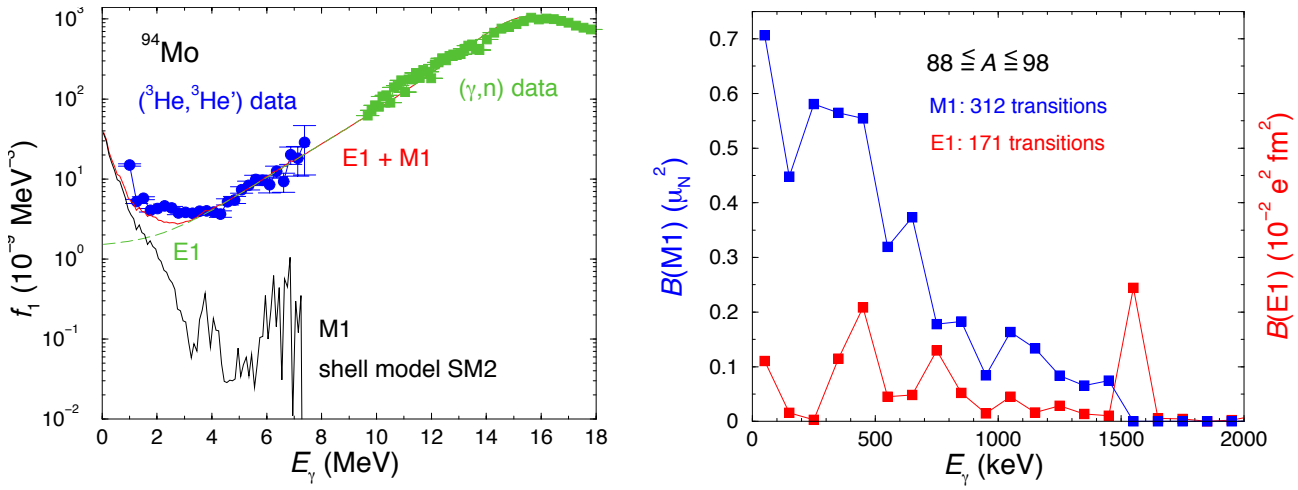

FIGURE 1. (Color online) **Left panel:** Strength functions for ^{94}Mo deduced from (^{3}He,^{3}He') (blue circles) and (γ,n) (green squares) experiments, the $M1$ strength function from the present Shell Model calculations (black solid line), $E1$ strength according to the GLO analytical expression (green dashed line), and the total $(E1+M1)$ dipole strength function (red line). **Right panel:** Average reduced transition probabilities of discrete dipole transitions in all nuclides with $88 \leq A \leq 98$ as reported in ENSDF [5]. The transitions are sorted into bins of 100 keV of the transition energy. Reprinted with permission from Ref. [1].

SHELL MODEL CALCULATIONS

The Shell Model calculations were performed within two model spaces. The first one (SM1) included the active proton orbits $\pi(0f_{5/2},1p_{3/2},1p_{1/2},0g_{9/2})$ and the neutron orbits $\nu(1p_{1/2},0g_{9/2},1d_{5/2})$ relative to a ^{66}Ni core. The second one (SM2) included the same proton orbits, but the active neutron orbits $\nu(0g_{9/2},1d_{5/2},0g_{7/2})$ relative to a ^{68}Ni core. We discuss only the results for (SM2), because the ones for (SM1) are very similar. Details about the set of empirical matrix elements for the effective interaction and of the single particle energies in this model space are given in Refs. [1, 6]. Our previous studies of nuclei with $N = 46-54$ demonstrated that the present Shell Model very well accounts for the experimental energies and transition probabilities of discrete states near the yrast line (see Ref. [6] and references therein). For calculating the reduced transition probabilities $B(M1)$ effective g-factors of $g_s^{\rm eff} = 0.7 g_s^{\rm free}$ have been applied.

To make the calculations feasible truncations of the occupation numbers were applied. In SM2, up to two protons could be lifted from the $1p_{1/2}$ orbit to the $0g_{9/2}$ orbit. In ^{94,95}Mo, one neutron from the $0g_{9/2}$ orbit could be excited to either the $1d_{5/2}$ or the $0g_{7/2}$ orbit, and one from the $1d_{5/2}$ to the $0g_{7/2}$ orbit. In ^{90}Zr, one neutron from the $0g_{9/2}$ orbit may be excited to the $1d_{5/2}$ orbit and one from the $1d_{5/2}$ orbit to the $0g_{7/2}$ orbit, or one neutron from the $0g_{9/2}$ orbit and one from the $1d_{5/2}$ orbit may be excited to the $0g_{7/2}$ orbit.

The calculations included states with spins from J = 0 to 6 for ^{90}Zr and ^{94}Mo and from J = 1/2 to 13/2 for ^{95}Mo. For each spin the lowest 40 states were calculated. The reduced transition probabilities $B(M1)$ were calculated for all transitions from initial to final states with energies $E_f < E_i$ and spins $J_f = J_i, J_i \pm 1$. For the minimum and maximum J_i, the cases $J_f = J_i - 1$ and $J_f = J_i + 1$, respectively, were excluded. This resulted in more than 14000 $M1$ transitions for each parity $\pi = +$ and $\pi = -$, which were sorted into 100 keV bins according to their transition energy $E_\gamma = E_i - E_f$. The average $B(M1)$ value for one energy bin was obtained as the sum of all $B(M1)$ values divided by the number of transitions within this bin. The results for ^{94}Mo are shown in Fig. 2 (left). They look quite similar for the other nuclides studied. Clearly there is a spike at zero energy that extends to about 2 MeV, which we call **Low-Energy MAgnetic Radiation (LEMAR).**

The inset of Fig. 2(left) demonstrates that, up to 2 MeV, the LEMAR spike of $\overline{B}(M1,E_\gamma)$ is well approximated by the exponential function

$$\overline{B}(M1,E_\gamma) = B_0 \exp(-E_\gamma/T_B), \tag{1}$$

with $B_0 = \overline{B}(M1,0)$ and T_B being constants. This is the case for all studied cases. For the respective parities $\pi = +,-$ we find for ^{90}Zr: B_0 = (0.36, 0.58) μ_N^2 and T_B = (0.33, 0.29) MeV, for ^{94}Mo: B_0 = (0.32, 0.16) μ_N^2 and T_B = (0.35, 0.51)

MeV, for ^{95}Mo: B_0 = (0.23, 0.12) μ_N^2 and T_B = (0.39, 0.58) MeV, and for ^{96}Mo: B_0 = (0.20, 0.13) μ_N^2 and T_B = (0.41, 0.50) MeV.

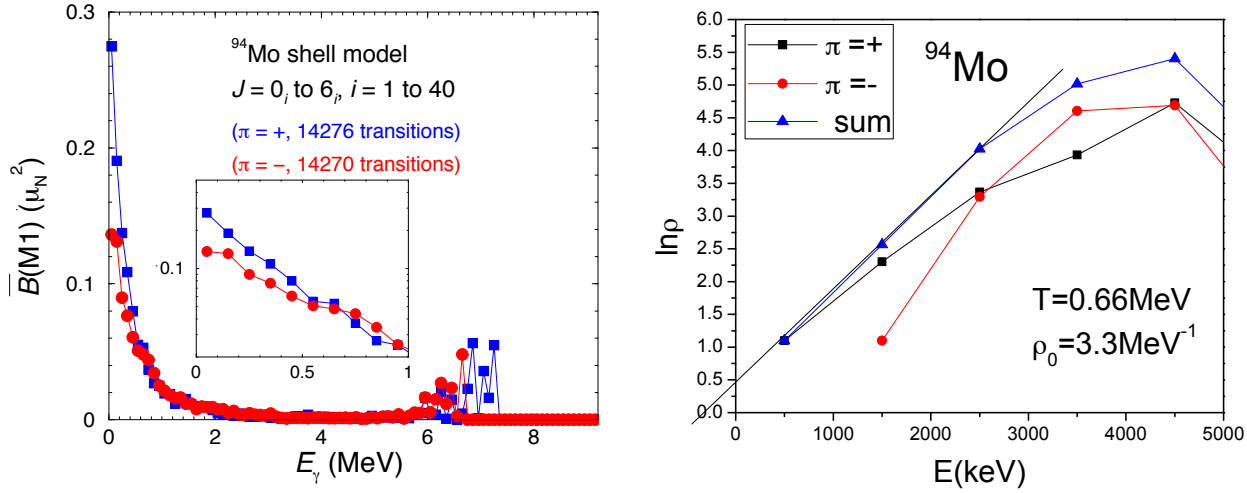

FIGURE 2. (Color online) **Left panel:** Average $B(M1)$ values in 100 keV bins of the transition energy calculated for positive-parity (blue squares) and negative-parity (red circles) states in ^{94}Mo. The inset shows the low-energy part in logarithmic scale. Reprinted with permission from Ref. [1]. **Right panel:** Level density of ^{94}Mo calculated as the number of levels within bins of 1 MeV.

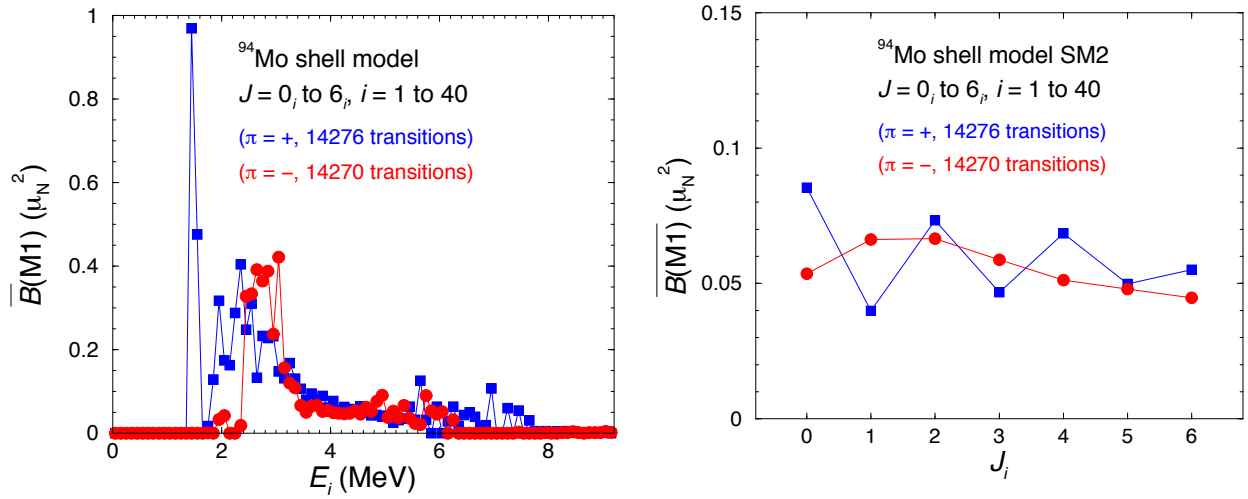
^{94}Mo shell model
$J = 0_i$ to 6_i, i = 1 to 40
(π = +, 14276 transitions)
(π = −, 14270 transitions)
$\overline{B}$(M1) (μ_N^2)
E_i (MeV)
^{94}Mo shell model SM2
$J = 0_i$ to 6_i, i = 1 to 40
(π = +, 14276 transitions)
(π = −, 14270 transitions)
$\overline{B}$(M1) (μ_N^2)
J_i

FIGURE 3. (Color online) **Left panel:** Average $B(M1)$ values in 100 keV bins of the excitation energy calculated for positive-parity (blue squares) and negative-parity (red circles) states in ^{94}Mo. **Right panel:** Average of the $B(M1)$ values for transitions originating from the lowest 40 initial state of given angular momentum J_i. Reprinted with permission from Ref. [1].

The exponential dependence on the transition energy is retained by the $M1$ strength functions, which are defined by the relation

$$f_{M1}(E_\gamma) = 16\pi/9(\hbar c)^{-3}\overline{B}(M1,E_\gamma)\rho(E_i), \tag{2}$$

where the level density at the initial state $\rho(E_i)$ is obtained from the Shell Model calculations. The level densities $\rho(E_i,\pi)$ were determined by counting the calculated levels within energy intervals of 1 MeV for the two parities separately. These combinatorial level densities were used in calculating the strength functions by means of Eq. (2). Fig. 2 (right) shows the level density for ^{94}Mo for both parities. As seen in Fig. 1 (left), there is a pronounced enhancement

below 2 MeV, which is well described by the exponential function

$$f_{M1}(E_\gamma) = f_0 \exp(-E_\gamma/T_f). \quad (3)$$

For ^{90}Zr, ^{94}Mo, ^{95}Mo, and ^{96}Mo, the parameters are f_0 = (34, 37, 39, 55) $\times$ 10^{-9} MeV^{-3} and T_f = (0.50, 0.50, 0.51, 0.48) MeV, respectively. The calculated M1- enhancement is consistent with the experiment, which however did not determine wether the radiation is electric or magnetic.

To find out which states generate strong $M1$ transitions, the average $\bar{B}(M1)$ values for ^{94}Mo are plotted as a function of the energy of the initial states in Fig. 3 (left). The $\overline{B}(M1)$ distributions versus E_i in ^{95}Mo and ^{96}Mo look similar to the ones in ^{94}Mo, but are shifted to somewhat lower excitation energy. In ^{90}Zr, the distributions start at about 3 MeV and continue to 10 MeV. Fig. 3 (right) shows that the transitions from initial states with different angular momentum within the studied range of $0 \leq J \leq 6$ have about the same probability. The distributions for the other nuclides are similar.

To summarize:

- **LEMAR is generated by a huge number of weak low-energy $M1$ transitions.**
- **They originate from high-lying states.**
- **They add up to strong $M1$ radiation.**
- **LEMAR accounts for the observed low-energy enhancement of the strength function.**

ORIGIN OF THE M1-STRENGTH

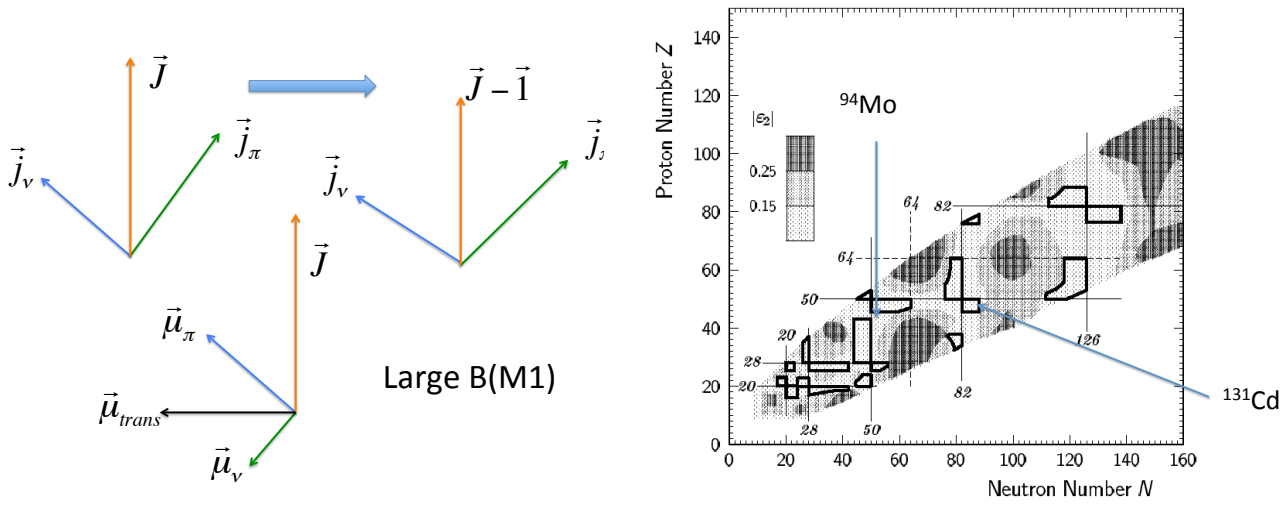

FIGURE 4. (Color online) **Left panel:**Magnetic Rotation as an example for large values of $B(M1)$ between two states generated by coupling the protons in one configuration ($\vec{j}_\pi$) and neutron holes in another configuration ($\vec{j}_\nu$) to total spin J and $J-1$. Semiclassically, $B(M1) \approx 3/8\pi\mu^2_{trans}$, because the transverse magnetic moment $\vec{\mu}_{trans}$ rotates about the axis $\vec{J}$ generating strong magnetic radiation. Along a rotational band the angular momenta of the protons and neutron holes gradually align against the repulsive residual interaction between the orbitals, which results in the regular spacing $\hbar\omega$ between the band members. The $M1$ radiation is very strong, because the $j = l + 1/2$ orbitals have large absolute values of the g-factors, and the transverse components of the magnetic moments $\vec{\mu}_\pi$ and $\vec{\mu}_\nu$ add, because $g_\pi > 0$ and $g_\nu < 0$. For details see Ref. [7]. **Right panel:** Regions where Magnetic Rotation is observed or predicted (inside the black boundaries). The conditions for appearance are: A combination of high-j proton particle orbitals with high-j neutron holes (or vice versa) and small deformation. Reprinted with permission from Ref. [7].

LEMAR is caused by transitions between many close-lying states of all considered spins located well above the yrast line in the transitional region to the quasi-continuum of nuclear states. Inspecting the composition of initial and final states, one finds large $B(M1)$ values for transitions between states that contain a large component (up to about 50%) of the same configuration with broken pairs of both protons and neutrons in high-j orbits. The largest $M1$

matrix elements connect configurations with the spins of high-j protons re-coupled with respect to those of high-j neutrons to the total spin $J_f = J_i, J_i \pm 1$. The main configurations are $\pi(0g_{9/2}^2)\nu(1d_{5/2}^2)$, $\pi(0g_{9/2}^2)\nu(1d_{5/2}^1 0g_{7/2}^1)$, and $\pi(0g_{9/2}^2)\nu(1d_{5/2}^2 0g_{9/2}^{-1} 0g_{7/2}^1)$ for positive-parity states in ^{94}Mo. Negative-parity states contain a proton lifted from the $1p_{1/2}$ to the $0g_{9/2}$ orbit in addition. The orbits in these configurations have large g-factors with opposite signs for protons and neutrons. Combined with specific relative phases of the proton and neutron partitions they cause large total magnetic moments.

For states near the yrast line, the re-coupling of spin generates the "Shears Bands" manifesting "Magnetic Rotation" (MR) [7], the mechanism of which is described in Fig. 4 (left). Regular MR bands are dominated by the configurations of $j = l + 1/2$ orbitals, which generate easily angular momentum and $M1$ radiation. MR was observed in the mass 90 region [8]. When less favorable orbtitals are an essential component of the configuration, the sequences become less regular (see e.g [9]). Typical transition energies are about 0.5 MeV both for the regular and irregular sequences.

The residual interaction between the valence particles and holes generates an energy difference between the states related to each other by recouping the angular momenta, which were degenerated without it. These energetic splittings enable transitions between the states by emitting an $M1$ γ-quant. In this sense, it is the residual interaction that generates the radiation. MR bands are located close to the yrast line. Accordingly, the configurations are rather pure, and the transition energies increase with angular momentum in a regular way. The high-lying states that generate the LEMAR are composed of a strong mix of configurations. The complex mixing changes the residual interaction between the states. As a consequence, the distance between the states becomes randomized. As discussed below, the mean transition energy of the LEMAR strength function is 0.5 MeV, which is the typical transition energy for MR bands.

To summarize:

- **LEMAR consists of transitions between states related by angular momentum recoupling of the same high-j proton and neutron configurations.**
- **Transition energies and probabilities are randomized.**
- **LEMAR is closely related to Magnetic Rotation.**

REGIONS WHERE LEMAR IS EXPECTED

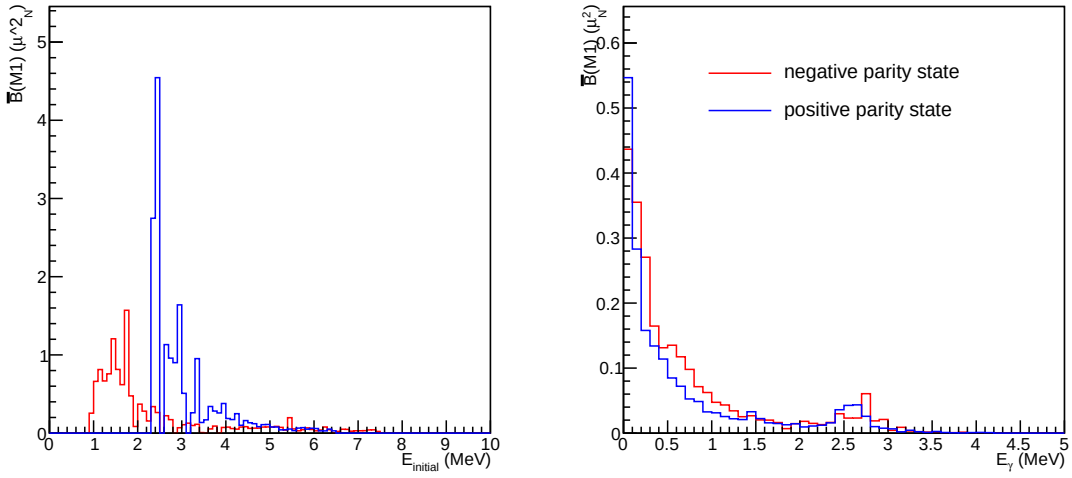

FIGURE 5. Right panel: Average $B(M1)$ values in 100 keV bins of the transition energy calculated for ^{131}Cd. Left panel: Average $B(M1)$ values in 100 keV bins of the excitation energy calculated for ^{131}Cd.

The close relation between MR and LEMAR suggests that both phenomena appear in the same nuclei. The regions in the nuclear chart, where MR is expected, are delineated in Fig. 4 (right). In fact, ^{90}Zr and the Mo isotopes discussed in the present work as well as the Fe, Ni, and Cd isotopes, for which the low-energy enhancement was observed, belong

to these regions. On the other hand, ^{117}Sn, ^{158}Gd, and the Th, Pa isotopes, for which no low-energy enhancement was observed, lie outside these regions (see Ref. [1] for references).

According to Fig. 4 (right), MR is predicted for the region with proton number below $Z = 50$ and neutron number above $N = 82$. These nuclei play a key role in the r-process of element synthesis in violent stellar events. For this reason we studied ^{131}Cd, which is a waiting point in the reaction chain. The Shell Model calculation was performed within the model space of the $1p_{3/2}$, $0f_{5/2}$, $1_{p1/2}$, $0g_{9/2}$ proton holes and $0h_{9/2}$, $1f_{7/2}$, $1f_{5/2}$, $2p_{3/2}$, $2p_{1/2}$ neutrons particles using a G-matrix derived from the CD-Bonn NN interaction. Fig. 5 shows the results, which are quite similar to the ones for the stable Mo isotopes. As demonstrated in Ref. [2], a low-energy enhancement of the dipole strength function comparable to the one observed in stable nuclei will substantially change the abundances of the elements synthesized in the r-process. Calculations of element abundances using γ-strength functions that include the LEMAR spike are on the way.

To summarize:

- **LEMAR is expected where MR appears.**
- **Nuclides with observed or missing low-energy enhancement in the γ-strength function correspond to the ones where LEMAR is expected.**
- **LEMAR is predicted is for ^{131}Cd.**
- **Strong modifications of the r-process rates are expected.**

STATISTICAL PROPERTIES OF THE TRANSITIONS

As the LEMAR is generated by a huge number of weak transitions between complex states, it is natural to study their statistical characteristics. The study is still on the way, and we report only tentative results obtained so far.

As already pointed out and illustrated by the left panel of Fig. 6, the average reduced transition probabilities $B(M1)$ decrease exponentially with the energy difference between initial and final states of the transitions. The decrease is determined by the parameter T_B in Eq. (1), which scatters around 0.5 MeV. The strength functions decrease exponentially as well, with the characteristic parameter in Eq. (3) $T_f \approx 0.5$ MeV. The mean value of the transition energy for the strength function is $T_f \approx 0.5$ MeV, which is the typical transition energy for MR. Such pronounced exponential dependence is unusual. More common are a weak dependence on the transition energy or a Lorentzian resonance caused by some doorway state (e. g. the Giant Dipole Resonance in the $E1$ strength function).

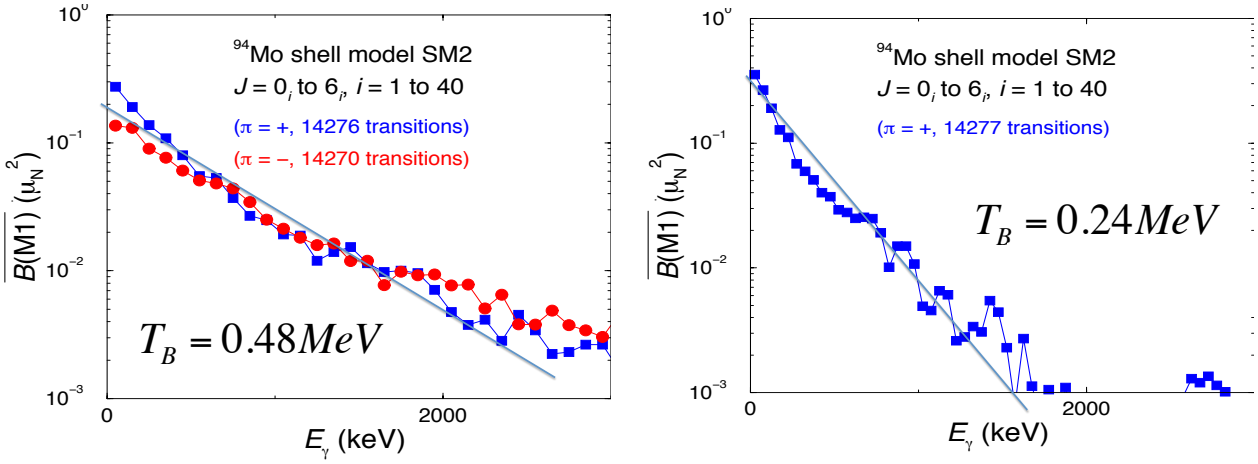
94Mo shell model SM2
J = 0_i to 6_i, i = 1 to 40
(π = +, 14276 transitions)
(π = –, 14270 transitions)
T_B = 0.48MeV
B(M1) (μ_N^2)
E_γ (keV)
94Mo shell model SM2
J = 0_i to 6_i, i = 1 to 40
(π = +, 14277 transitions)
T_B = 0.24MeV
B(M1) (μ_N^2)
E_γ (keV)

FIGURE 6. (Color online) Average $B(M1)$ values in 100 keV bins of the transition energy calculated for positive-parity (blue squares) and negative-parity (red circles) states in ^{94}Mo. **Left panel:** full interaction, **Right panel:** half interaction

Fig. 2 (right) shows that the total level density $\rho(E_i)$ is well reproduced by the constant-temperature expression

$$\rho(E_i) = \rho_0 \exp(E_i/T_\rho) \tag{4}$$

as long as $E_i < 3$ MeV. For higher energies the combinatorial level density deviates from this expression and eventually decreases with excitation energy, which is obviously due to missing levels at high energy in the present configuration space. The level densities for ^{95,96}Mo are similar. From a fit to the combinatorial values in the range $E_i < 2$ MeV we found for (ρ_0, T_ρ) in (MeV^{-1}, MeV) the values of (1.37, 0.67), (1.90, 0.54), and (1.25, 0.58) for ^{94}Mo, ^{95}Mo, and ^{95}Mo, respectively. The level density in the semi-magic ^{90}Zr shows a more complicated energy dependence. It is noticed that the micro canonical temperature $T_\rho \sim 0.6$ MeV, is close to $T_M \sim 0.5$ MeV, which determines the exponential decrease of the average $B(M1)$ values with the transition energy.

The size distribution of the $B(M1)$ values is shown in Fig. 7. Based on Shell Model [10] and experimental [11] studies of γ- transitions between complex excited states, we expected a Porter-Thomas-like distribution. As seen in the left panel, our distribution turned out to be very different. Also the more general $\chi^2(y,\nu)$ distributions for various indices ν do not account for our distribution. Quite surprisingly, we found that the distribution follows a power law

$$P(y) = Ay^\nu \quad y = B(M1)/\overline{B(M1)}, \tag{5}$$

which is illustrated by the right panel. Here, $\overline{B(M1)}$ is the mean value over the complete distribution. The distributions for both parities in all three nuclides follow a power law with the exponents ν scattering around 1.2.

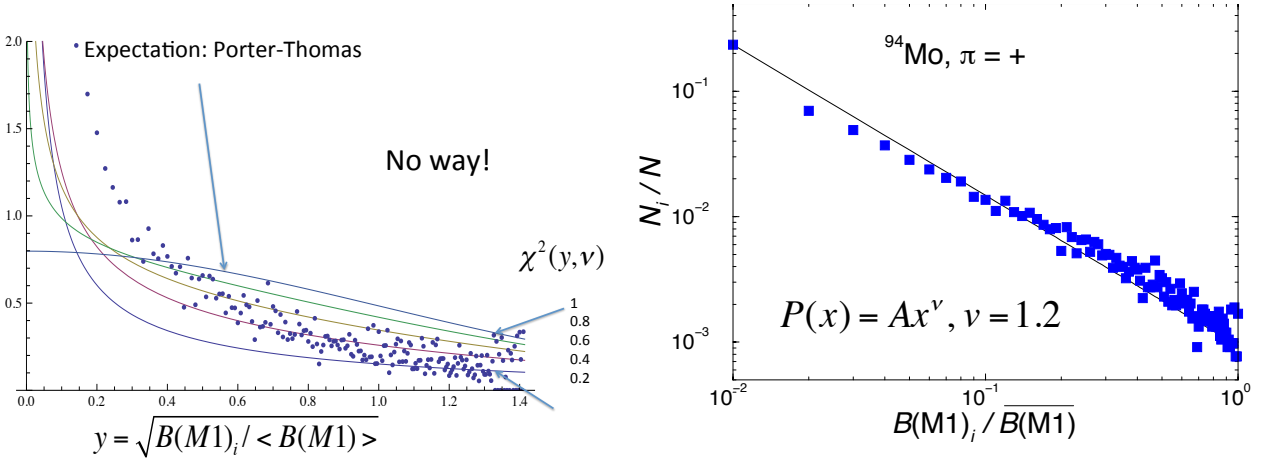

FIGURE 7. (Color online) **Left panel:** Probability distribution of the $B(M1)$ values in ^{94}Mo for positive parity states compared with χ^2 distributions of different index ν, where $\nu = 1$ is the Porter-Thomas distribution. **Right panel:** Probability distribution of the $B(M1)$ values in ^{94}Mo for positive parity states compared with a power law distribution (straight line).

The Porter-Thomas distribution characterizes the Gaussian Orthogonal Ensemble (GOE) of random matrices (see Ref. [12] for a recent review). Its appearance is taken as a signature of onset of many-body chaos in a quantum system, in which time reversal symmetry is conserved. The LEMAR distribution of the $B(M1)$ values deviates drastically from the GOE. The reason may be the fact that LEMAR is generated by the subset of transitions between special states that are related by re-coupling of angular momentum. These states have the same energy without residual interaction. In contrast, the orthogonality condition of the GOE requires that its random matrices have Gaussian probability distributions for both the diagonal and the non-diagonal matrix elements, where the width of the former is twice the width of the latter. As discussed in Ref. [13], it may also be that the considered valence space and the sampled range of excitation energies are too small for approaching the chaotic regime.

The fact that the LEMAR distributions can be described by a simple power law is remarkable in our view. So far we have not found a conclusive explanation. Power-law distributions are characteristic for scale-free systems, as for example the distribution of the number of clicks/site in the internet (Any site can connect with any number of other sites.) or the heat capacity near a second order phase transition (There is no scale for the fluctuations of the order parameter.). LEMAR may be classified as scale-free as follows. The various configurations that are related by re-coupling of the angular momentum have all the same energy. The energy difference between the mixed states is generated by their residual interaction, which acts in a random way between the complex states. This differs from the conventional situation, where the single particle level spacing represents an energy scale for the various configurations to mixed by the residual interaction.

Statistical self-similarity is another signature of scale-free systems. It means that the statistical characteristics of the system are the same when studied on different scales (The length of coast lines is a popular example.). LEMAR seems to exhibit statistical self-similarity. The right panel of Fig. 6 shows the average $B(M1)$ values calculated within the same model space and multiplying each matrix element of the residual interaction by a factor of 0.5 (i. e. changing the scale). Comparing with the results for the full interaction in in the left panel, it is seen that the distribution remains exponential, where the characteristic parameter $T_B = 0.24$ MeV is one half of $T_B = 0.48$ MeV of the full calculation.

Finally, we remark that the exponential growth of the low-energy level density with excitation energy has been attributed to the quenching of the pairing correlations, which corresponds to the phase transition of second order observed in macroscopic superconductors and supra fluids. Magnetic transitions are known to be sensitive to the presence of pair correlations. It is possible that the phenomena are related, and the closeness of the parameters $T_\rho \sim T_B \sim 0.5$ MeV is more than accidental.

To summarize:

- **The LEMAR strength function decreases exponentially with increasing transition energy.**
- **The combinatorial level density increases exponentially with the excitation energy.**
- **The two parameters that control the respective decay or growth are $T_B \sim T_\rho \sim 0.5$ MeV.**
- **The size distribution of the reduced transition probabilities is a power law with an exponent of ~ 1.2.**
- **LEMAR representing a scale-free system might be the reason for these unexpected statistcal properties.**

Our considerations concerning the exponential decrease of the LEMAR strength function and of the power law of the $B(M1)$ size are speculative so far. A more profound analysis is on the way, which may provide a better understanding of the nature and origin of these unexpected phenomena.

ACKNOWLEDGMENTS

Supported by the Grant No. DE-FG02-95ER4093 of the US Department of Energy.

REFERENCES

1. R. Schwengner, S. Frauendorf,A. C. Larsen, *Phys. Rev. Lett.* **111**, 232504 (2013)
2. A. C. Larsen and S. Goriely, *Phys. Rev. C* **82**, 014318 (2010).
3. M. Guttormsen *et al.*, *Phys. Rev. C* **71**, 044307 (2005).
4. N. Pietralla *et al.*, *Phys. Rev. Lett.* **83**, 1303 (1999).
5. http://www.nndc.bnl.gov/nudat2/
6. R. Schwengner *et al.*, *Phys. Rev. C* **8**0, 044305 (2009).
7. S. Frauendorf, *Rev. Mod. Phys.* **7**3, 463 (2001).
8. H. Schnare *et al.*,*Phys. Rev. Lett.* **8**2, 4408 (1999).
9. S. Frauendorf, J. Reif ,*Nucl. Phys. A* **6**21, 736 (1997).
10. A. Hamoudi *et al.*, *Phys. Rev. C* **6**5, 064311 (2002).
11. J. F. Shriner *et al.*, *Phys. Rev. C* **6**2, 054305 (2002)
12. H. Weidenmüller and G. Mitchell, *Rev. Mod. Phys.* **8**1, 539 (2009). .
13. V Zelevinsky and A. Volya, *Phys. Rep.* **3**91, 311 (2004). .